Effect of fluctuations on the Hall effect and thermomagnetic effects in a superconductor near its transition temperature

A. A. Varlamov and D. V. Livanov

Moscow Institute of Steel and Alloys
(Submitted 12 March 1990)
Zh. Eksp. Teor. Fiz. **99**, 1816–1826 (June 1991)

The influence of superconducting fluctuations on the Hall effect and thermomagnetic effects in a superconductor near its transition temperature is analyzed. The case of a quasi-2D electron spectrum is examined for comparison with experimental data on high T_c superconductors. Incorporating superconducting fluctuations results in the appearance of anomalies on the temperature dependence of the Hall, Nernst, Ettinghausen, and Righi–Leduc coefficients near T_c. These predictions agree with the results of recent experiments on high T_c superconductors.

1. INTRODUCTION

The multifaceted research on the high T_c superconductors and the synthesis of high-quality samples have increased research interest in such subtle effects as galvanomagnetic and thermomagnetic effects. The Hall effect has been the subject of the most active research in recent years. It has been pointed out in several papers that the Hall conductivity behaves anomalously near the transition temperature. In particular, there is a peak in its temperature dependence at the transition from the normal phase to the superconducting phase.[1-3]

Just recently, on top of the general increase in interest in heat transfer in the high T_c superconductors, along with the active research on the thermal emf and the thermal conductivity several studies on the behavior of these coefficients in a magnetic field (i.e., on the Nernst, Ettinghausen, and Righi–Leduc effects) have appeared.[4-7] These studies have revealed clearly defined peaks on the temperature dependence of the Nernst and Ettinghausen coefficients at the threshold of the superconducting transition. The temperature dependence of the thermal conductivity in a magnetic field was also studied in Ref. 7. It was found that as T_c is approached from above the decrease in the Righi–Leduc coefficient gives way to an increase a few degrees away from T_c. There are thus anomalies near the transition temperature in the behavior of the kinetic coefficients corresponding to all galvanomagnetic and thermomagnetic effects. These results suggest that superconducting fluctuations are strongly influencing the kinetic properties of the high T_c superconductors.

At the same time, the validity of the description of heat-transfer processes in systems of interacting particles has recently become the topic of a widespread debate. As a result, a systematic method has been formulated for calculating the kinetic coefficients associated with heat transfer from the Kubo-Greenwood formulas.[8,9] This method was used in Ref. 9 to calculate the fluctuational corrections to the thermal emf and the thermal conductivity of a superconductor at the threshold of the transition to the superconducting state. It was thus found possible to explain the peak observed on the temperature dependence of these thermal emf.

In the present paper we extend this approach to the calculation of the kinetic coefficients which describe the transport of heat and electric charge in a weak magnetic field. As a result, we examine the effect of superconducting fluctuations on the Hall effect and on various thermomagnetic effects in a superconductor at temperatures slightly above the transition temperature. With an eye toward the use of this theory to explain the experimental results on layered high T_c single crystals, and in view of the short correlation length in these materials, we follow Refs. 9 and 10 in adopting the model of a layered clean superconductor with a quasi-2D electron spectrum. As we will see below, superconducting fluctuations are important in the galvanomagnetic and thermomagnetic effects over a fairly broad temperature range near T_c. They may be responsible for the anomalies found experimentally on the temperature dependence of the corresponding kinetic coefficients.

In Sec. 2 we formulate a linear-response method for calculating the kinetic coefficients describing transport in a weak magnetic field. Here we make use of a temperature Feynman-diagram technique. In Sec. 3 we take this approach to calculate the kinetic coefficients of a normal layered metal. In Secs. 4–6 we discuss the influence of superconducting fluctuations, and we calculate the fluctuational corrections to the Hall conductivity and to the Nernst, Ettinghausen, and Righi-Leduc coefficients. The results are discussed in the Conclusion, where the success of these results in explaining experimental data is also discussed.

2. GALVANOMAGNETIC AND THERMOMAGNETIC EFFECTS IN WEAK FIELDS. FEYNMAN-DIAGRAM APPROACH

Before we start our discussion of the effect of superconducting fluctuations on the Hall effect and thermomagnetic effects in a superconductor near its transition temperature, and before we calculate the corresponding kinetic coefficients, we would like to discuss the general approach to this problem within the framework of a temperature Feynman-diagram technique. Here we are following Refs. 11 and 12, where a similar approach was taken to study the Hall effect in a disordered 2D electron gas.

In a weak electric field and a magnetic field, with a low temperature gradient (low enough that we can restrict the analysis to terms of first order in the variations), generalized transport equations for the current and the heat flux can be written[13]

$$\begin{aligned}\mathbf{j}&=\sigma\mathbf{E}+\sigma_H[\mathbf{EH}]+\beta\nabla T+N[\nabla T,\mathbf{H}],\\ \mathbf{q}&=\gamma\mathbf{E}+B[\mathbf{EH}]-\varkappa\nabla T+L[\nabla T,\mathbf{H}],\end{aligned}\tag{1}$$

 0038-5646/91/061016-07$03.00

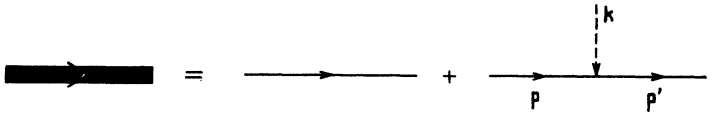

FIG. 1. Green's function of an electron with an interaction with a weak magnetic field.

where **E**, **H**, and ∇T are the electric field, the magnetic field, and the temperature gradient, respectively; σ is the electrical conductivity, σ_H is the Hall conductivity, β is a thermoelectric coefficient, N is the Nernst coefficient, $\gamma = -\beta T$, B is the Ettinghausen coefficient, $\varkappa$ is the thermal conductivity, and L is the Righi–Leduc coefficient.

Any of the kinetic coefficients in (1) can be expressed in terms of the correlation functions of two flux operators (electrical or thermal).[14,15] In a Feynman-diagram representation, this approach reduces to calculating the loops of exact one-electron Green's functions with corresponding external field vertices: electric, $(e/m)(\mathbf{A}_e\mathbf{p})$, or thermal, $(\xi_p/m)(\mathbf{A}_q\mathbf{p})$ ($i\Omega\mathbf{A}_e = \mathbf{E}$, $i\Omega\mathbf{A}_q = \nabla T$, e, and m are the charge and mass of an electron, $\mathbf{p}$ is half the sum of the momenta corresponding to the Green's functions which form the loop, and ξ_p is the electron energy reckoned from the Fermi level and corrected for various types of interactions[9]).

While the magnetic field can be assumed to be zero (i.e., corrections arise only in second order in the field) over a wide range in the calculations of σ, β, γ, and $\varkappa$, in the calculation of the coefficients σ_H, N, B, and L the electron Green's functions should incorporate the interaction of the electron with the magnetic field. In the case at hand, of a weak field ($eH\tau/mc \ll 1$, where τ is the relaxation time of the electron's momentum, and c is the velocity of light), it is sufficient to work in first-order perturbation theory (Fig. 1). The vertex describing the interaction of the electron with the magnetic field is $(e/2m)(\mathbf{A}_H, \mathbf{p}+\mathbf{p}')$, where $i[\mathbf{k}\mathbf{A}_H] = \mathbf{H}$, and $\mathbf{k}$ is the wave vector of the magnetic field.

In calculating the kinetic coefficients describing transport in a weak magnetic field, we should thus consider a loop of three free one-electron Green's functions (without a magnetic field) with three vertices. Two of the vertices correspond to flux operators, while the third reflects the interaction of the electron with the static magnetic field applied to the system.

3. CASE OF A LAYERED METAL IN THE NORMAL PHASE

To illustrate the approach taken above, we consider the calculation of the coefficients which we need for a metal in its normal phase. Keeping in mind our goal below—to study fluctuation effects in a high T_c superconductor—we discuss a model of a layered metal with a corrugated-cylinder Fermi surface.[16] In this case the electron spectrum is

$$\xi_p = \varepsilon_p - \varepsilon_F = v_F(|\mathbf{p}_\parallel| - p_F) + w\cos(p_\perp a), \qquad (2)$$

where v_F, p_F, and ε_F are the Fermi velocity, momentum, and energy in the plane of a layer, w is the overlap integral, which is a measure of the probability for jumping of electrons between layers, a is the interlayer distance, and $\mathbf{p} = (\mathbf{p}_\parallel, p_\perp)$ is the quasimomentum of the electron.

In the case of an anisotropic spectrum, the kinetic coefficients in (1) are generally tensors. In a layered metal, however, we are interested in only those components of the fluxes **j** and **q** which lie in the plane of a layer (the *ab* plane in Fig. 2), since the fluxes in the direction normal to the plane of the layer are suppressed by the small overlap integral. The corresponding kinetic coefficients are thus small quantities, with a relative order of magnitude

$$\left(\frac{wa}{v_F}\right)^2 \ll 1.$$

We assume that the magnetic field is directed parallel to the c axis and that the electric field and the temperature gradient lie in the *ab* plane.[1)] The motion of the electrons in the plane of the layers is then isotropic. By virtue of the arguments above, we can thus assume that the kinetic coefficients in (1) are scalars.

We begin with the Hall effect. According to (1), the Hall current is proportional to the quantity

$$[\mathbf{EH}] = \Omega[\mathbf{A}_H(\mathbf{k}\mathbf{A}_e) - \mathbf{k}(\mathbf{A}_H\mathbf{A}_e)]. \qquad (3)$$

We can simplify the calculations by adopting the gauge condition[12] $\mathbf{k}\cdot\mathbf{A}_H = 0$. Consequently, we will be interested below in only those terms which are proportional to the first term in (3).

The resulting diagrams are shown in Fig. 3. In calculating the Hall current, we need to associate the expressions $(e/m)\mathbf{p}$ and $(e/m)(\mathbf{A}_e\mathbf{p})$ and with the external vertices. The solid lines correspond to the Green's functions of a normal metal with spectrum (2):

$$G(\mathbf{p}, \varepsilon_n) = (i\tilde{\varepsilon}_n - \xi_p)^{-1}, \quad \tilde{\varepsilon}_n = \varepsilon_n + \frac{1}{2\tau}\operatorname{sgn}\varepsilon_n,$$

$$\varepsilon_n = 2\pi T(n+{}^1/_2). \qquad (4)$$

Since we are interested in terms of first order in **k**, we should expand the Green's functions which depend on this momentum. An expression for the Hall current which incorporates both of the diagrams in Fig. 3 is

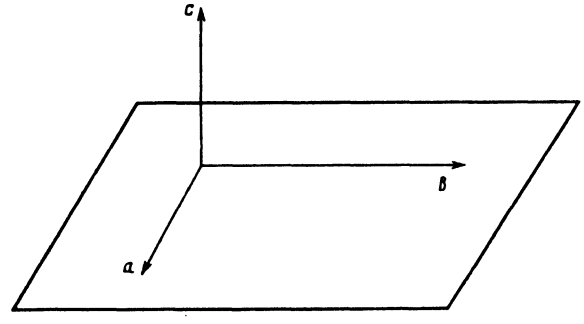

FIG. 2. Orientation of the coordinate axes with respect to the plane of a layer in a layered metal.

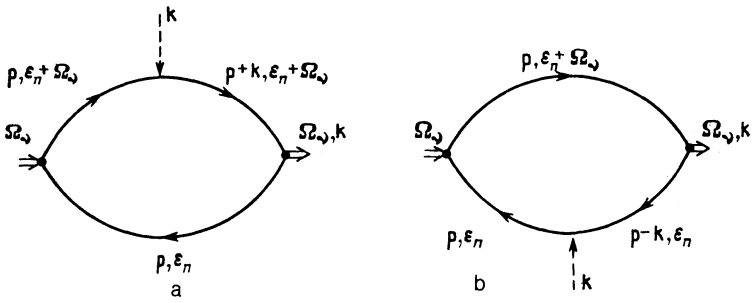

FIG. 3. Feynman diagrams describing the contributions to the kinetic coefficients of a normal metal.

$$\mathbf{j}_H = e^3 T \sum_{\varepsilon_n} \int (dp)\,[G^3(\mathbf{p},\varepsilon_n)G(\mathbf{p},\varepsilon_n+\Omega_\nu) + G(\mathbf{p},\varepsilon_n)G^3(\mathbf{p},\varepsilon_n+\Omega_\nu)]\,\mathbf{R}, \tag{5}$$

where we have separated the integral over the angles of the vector $\mathbf{p}$:

$$\mathbf{R} = \int \frac{d\Omega_p}{2\pi}(\mathbf{A}_e\mathbf{v})(\mathbf{A}_H\mathbf{v})(\mathbf{k}\mathbf{v})\mathbf{v} = \frac{v^4}{8}(\mathbf{A}_H(\mathbf{k}\mathbf{A}_e)+\mathbf{A}_e(\mathbf{k}\mathbf{A}_H)+\mathbf{k}(\mathbf{A}_H\mathbf{A}_e)). \tag{6}$$

As we have already mentioned, we are interested in only the first term. In the next approximation in ξ_p in (5), we need to carry out an expansion of the quantities which depend on the electron energies (the state density ρ and v^2) near the Fermi surface in order to obtain a nonvanishing result. We find

$$\mathbf{j}_H = \frac{e^3}{4} v^2 \left[\frac{\partial(\rho v^2)}{\partial\varepsilon}\right]_{\varepsilon_F} \tau^2 \Omega \mathbf{A}_H(\mathbf{k}\mathbf{A}_e), \tag{7}$$

from which we then find

$$\sigma_H^{(n)} = \frac{e^3}{4} v^2 \left[\frac{\partial(\rho v^2)}{\partial\varepsilon}\right]_{\varepsilon_F} \tau^2. \tag{8}$$

In calculating the Nernst coefficient we should put the vertices $(e/m)\mathbf{p}$ and $(\xi_p/m)(\mathbf{A}_q\mathbf{p})$ in the diagrams in Fig. 3. The heat-flux operator, along with the term describing the heat transfer by noninteracting electrons $(\xi_p\mathbf{v})$, also contains corrections for the interaction of the electrons with impurity centers and with a magnetic field under these conditions. In principle, the Feynman diagrams corresponding to those corrections should also be taken into consideration. However, calculations show that the contributions from these diagrams to the coefficients $N^{(n)}$ and $L^{(n)}$ cancel out with the contributions which come from the diagrams in Fig. 3 with the vertex $\xi_p\mathbf{v}$ in the case in which ξ_p reaches a value on the order of τ^{-1} in the pole integration. Consequently, only the same diagrams in Fig. 3 contribute to the Nernst and Righi–Leduc coefficients, since ξ_p becomes the electron frequency ε_n in the course of the integration.

In calculating the Nernst coefficient, which is proportional to

$$[\nabla T, \mathbf{H}] = \Omega\,[\mathbf{A}_H(\mathbf{k}\mathbf{A}_q) - \mathbf{k}(\mathbf{A}_H\mathbf{A}_q)],$$

we are interested in only the first term, as before. The presence of the additional energy ξ_p at the vertex makes it unnecessary to expand ρv^2 in the course of the integration over ξ_p. As a result we find

$$N^{(n)} = (\pi/4)\,e^2 v^4 \rho \tau^3 T. \tag{9}$$

Since the vertices are of the form $(\xi_p/m)\mathbf{p}$ and $(\xi_p/m)(\mathbf{A}_q\mathbf{p})$, we find the following expression for the Righi–Leduc coefficient:

$$L^{(n)} = \frac{\pi^2}{9} e v^2 \left[\frac{\partial(\rho v^2)}{\partial\varepsilon}\right]_{\varepsilon_F} \tau^2 T. \tag{10}$$

Although expressions (8)–(10) were derived for the case of a quasi-2*D* electron spectrum, they can easily be generalized to the case of metal with an isotropic spectrum. An additional factor of 2/3 appears in (8)–(10) in this case, reflecting the 3*D* nature of the angular integration.

4. INCORPORATION OF SUPERCONDUCTING FLUCTUATIONS

Before we proceed to the direct calculation of the effect of fluctuations on the kinetic coefficients of interest, we have a few important comments. First, there is the question of whether to choose the model of a clean superconductor ($T\tau \gg 1$) or that of a dirty superconductor ($T\tau \ll 1$). Since experiments on the high T_c superconductors show that an intermediate case ($T\tau \approx 1$) usually holds in real systems, it is our position that choosing one of the two limiting cases is a matter to be governed by convenience and simplicity in the calculations. Since the clean-case analysis simplifies the calculations substantially and reduces the number of diagrams to be taken into account, we assume below that the superconductor is clean.

A second question concerns the choice of a model for the electron spectrum. As we mentioned earlier, we are assuming a quasi-2*D* spectrum. This assumption is justified by the circumstance that most of the high T_c superconductors which are presently under study have a layered structure. Furthermore, we will automatically obtain the results for the 2*D* and 3*D* regimes in the behavior of the fluctuations (in the limiting cases of strong and weak coupling between layers).

As was shown above, in order to deal with the effect of superconducting fluctuations on the Hall effect and thermomagnetic effects, we need to add a vertex representing the interaction of the electrons with the magnetic field to the standard diagrams describing the fluctuational corrections to the electrical and thermal conductivities and the thermal emf.[9,17] The number of diagrams which arise as a result of this procedure turns out to be rather large. This point be-

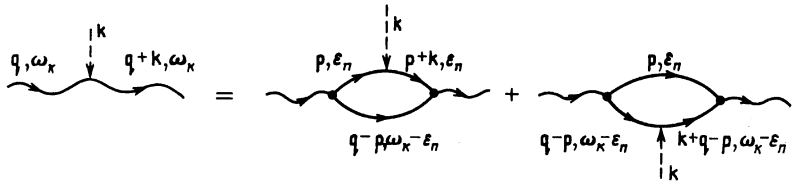

FIG. 4. Vertex representing the interaction of an electron with a magnetic field. The use of this vertex leads to the major contribution to the kinetic coefficients.

comes particularly obvious in a calculation of the kinetic coefficients associated with heat transfer, since it is necessary to take account of the corrections to the heat-flux operator for the magnetic field and the interelectron interaction.[9] However, the situation simplifies greatly because the contribution which is the most singular in terms of the degree of proximity to T_c comes from only those diagrams which arise when a vertex with a magnetic field is introduced in the Aslamazov–Larkin diagram, and then only that from the version of these diagrams in which the magnetic field "goes into" the fluctuation propagator. This propagator is given by the following expression near T_c, in the clean case, and with spectrum (2):

$$L(\mathbf{q},\omega_k)=-\frac{1}{\rho}\left[\frac{T-T_c}{T_c}+\frac{\pi\omega_k}{8T_c}+\frac{3}{2}\eta q_\parallel^2+6\eta\frac{w^2}{v^2}\sin^2\frac{q_\perp a}{2}\right]^{-1}, \tag{11}$$

where

$$\eta=\frac{7\zeta(3)v_F^2}{48\pi^2T_c^2}$$

[$\zeta(x)$ is the zeta function].

The simplest way to see what this vertex looks like is to write the fluctuation propagator as a set of electron loops, into one of which the magnetic field goes (in two possible ways) (Fig. 4).

The vertex of interest here can then be expressed in terms of blocks of Green's functions which have been calculated repeatedly:

$$\frac{eT}{m}\sum_{\varepsilon_n}\int(dp)[G(\mathbf{p},\varepsilon_n)G(\mathbf{p}+\mathbf{k},\varepsilon_n)G(\mathbf{q}-\mathbf{p},\omega_k-\varepsilon_n)(\mathbf{A}_H\mathbf{p})$$
$$+G(\mathbf{p},\varepsilon_n)G(\mathbf{q}-\mathbf{p}+\mathbf{k},\omega_k-\varepsilon_n)G(\mathbf{q}-\mathbf{p},\omega_k-\varepsilon_n)$$
$$\times(\mathbf{A}_H,\mathbf{q}-\mathbf{p})]=M(\mathbf{A}_H\mathbf{q}), \tag{12}$$

where

$$M=-\frac{7\zeta(3)}{8\pi^4}\frac{ep_F^3}{mT_c^2}. \tag{13}$$

We turn now to a direct calculation of the kinetic coefficients in which we are interested.

5. HALL EFFECT

The diagrams which make the major contribution to the Hall current (the contribution which is most singular in the degree of proximity to T_c) is shown in Fig. 5. The contribution of the first of these diagrams is

$$\mathbf{j}_H^{(a)}=\frac{2e^3M}{m}T\sum_{\omega_k}\int(dq)(\mathbf{A}_H\mathbf{q})(\mathbf{A}_e\mathbf{k})\mathbf{q}B_1B_2L(\mathbf{q},\omega_k+\Omega_\nu)$$
$$\times L(\mathbf{q}+\mathbf{k},\omega_k+\Omega_\nu)L(\mathbf{q},\omega_k), \tag{14}$$

$$\mathbf{q}B_1=T\sum_{\varepsilon_n}\int(dp)G(\mathbf{p},\varepsilon_n)G(\mathbf{p},\varepsilon_n+\Omega_\nu)G(\mathbf{q}-\mathbf{p},\omega_k-\varepsilon_n)\mathbf{v}, \tag{15}$$

$$(\mathbf{A}_e\mathbf{k})B_2=T\sum_{\varepsilon_n}\int(dp)G(\mathbf{p}+\mathbf{k},\varepsilon_n+\Omega_\nu)G$$
$$\times(\mathbf{p},\varepsilon_n)G(\mathbf{q}-\mathbf{p},\omega_k-\varepsilon_n)(\mathbf{A}_e\mathbf{v}). \tag{16}$$

Near the transition temperature we can ignore the dependence of blocks B_1 and B_2 on the fermion and boson frequencies, and we can treat these blocks as constants. To obtain the first order in $\mathbf{k}$ in the calculation of B_1 as a result, we should expand the Green's function $G(\mathbf{q}-\mathbf{p},\ \omega_k-\varepsilon_n)$, while in the calculation of B_2 we should expand $G(\mathbf{p}+\mathbf{k},\ \varepsilon_n+\Omega_\nu)$. We immediately note that in order to derive a nonvanishing result for the total Hall current (i.e., with the second diagram in Fig. 5 also being taken into account), we should expand the quantity ρv^2 near the Fermi surface in (15)–(16). After some straightforward calculations we find

$$B_1=\frac{7\zeta(3)}{4\pi^2}\frac{\rho v_F^2}{T_c^2}+\frac{i}{64T_c}\left[\frac{\partial(\rho v^2)}{\partial\varepsilon}\right]_{\varepsilon_F},\quad B_2=-B_1. \tag{17}$$

Substituting (17) into (14), and integrating over the angles of the vector $\mathbf{q}$,

$$\int\frac{d\Omega_p}{2\pi}(\mathbf{A}_e\mathbf{q})\mathbf{q}=\tfrac{1}{2}\mathbf{A}_eq_\parallel^2, \tag{18}$$

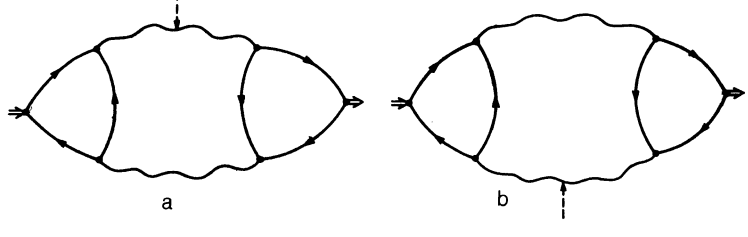

FIG. 5. Diagrams which dominate the fluctuational corrections to the kinetic coefficients.

we can calculate the contribution from the second diagram in Fig. 5 in a corresponding way:

$$\mathbf{j}_H=\mathbf{j}_H^{(a)}+\mathbf{j}_H^{(b)}=-\frac{i7\zeta(3)}{128\pi^2}\frac{e^3v_F^2\rho}{mT_c^3}\left[\frac{\partial(\rho v^2)}{\partial\varepsilon}\right]_{\varepsilon_F}\mathbf{A}_H(\mathbf{A}_e\mathbf{k})$$
$$\times T\sum_{\omega_k}\int(dq)\mathbf{q}_\parallel^2[L^2(\mathbf{q},\omega_k+\Omega_v)L(\mathbf{q},\omega_k)$$
$$-L(\mathbf{q},\omega_k+\Omega_v)L^2(\mathbf{q},\omega_k)]. \qquad (19)$$

Reducing the sum over ω_k in (19) to a contour integral, carrying out an analytic continuation in the standard manner,[17] and integrating over frequency, we find, to first order in $\Omega=i\Omega_v$,

$$\mathbf{j}_H=\frac{7\zeta(3)}{2^{11}\pi}\frac{e^3v_F^2}{\rho^2mT_c^3}\left[\frac{\partial(\rho v^2)}{\partial\varepsilon}\right]_{\varepsilon_F}\Omega\mathbf{A}_H(\mathbf{A}_e\mathbf{k})$$
$$\times\int(dq)\mathbf{q}_\parallel^2\left[\frac{T-T_c}{T_c}+{}^3/_2\eta q_\parallel^2+\delta_0^2\sin^2\frac{q_\perp a}{2}\right]^{-4}, \qquad (20)$$

where the parameter

$$\delta_0^2=\frac{7\zeta(3)w^2}{8\pi^2T_c^2}$$

is a measure of the extent to which the situation is quasi-two-dimensional. This parameter determines the effective dimensionality of the fluctuations.[16] Finally, integrating over momentum within one period of the corrugated cylinder in (20), and using (8), we find the correction to the Hall conductivity which we need:

$$\frac{\sigma_H^{(fl)}}{\sigma_H^{(n)}}=\frac{\pi}{18\cdot7\zeta(3)}\frac{1}{T_c\tau}\frac{1}{\varepsilon_F\tau}F\left(\frac{T-T_c}{T_c},\delta_0^2\right), \qquad (21)$$

where

$$F\left(\frac{T-T_c}{T_c},\delta_0^2\right)=\left(2\frac{T-T_c}{T_c}+\delta_0^2\right)\left[\frac{T-T_c}{T_c}\left(\frac{T-T_c}{T_c}+\delta_0^2\right)\right]^{-1/2}$$
$$=\begin{cases}\dfrac{1}{\delta_0}\left(\dfrac{T_c}{T-T_c}\right)^{1/2}, & \delta_0^2\gg\dfrac{T-T_c}{T_c},\\ 2\left(\dfrac{T_c}{T-T_c}\right)^2, & \delta_0^2\ll\dfrac{T-T_c}{T_c}.\end{cases} \qquad (22)$$

The two limiting cases which have been distinguished in (22) describe the 3*D* and 2*D* regimes, respectively, of the behavior of the fluctuations. At $T-T_c\sim\delta_0^2T_c$, the size of a fluctuational Cooper pair in the direction transverse with respect to the layers becomes comparable to the distance between layers, and the temperature dependence changes from three-dimensional to two-dimensional. Because of our use of the vertex in Fig. 4, the fluctuational correction to the Hall conductivity is more singular in the degree of proximity to T_c than is the correction to the conductivity in the absence of a magnetic field.[17]

6. THERMOMAGNETIC EFFECTS

We begin with the Nernst effect. The fluctuational correction to the Nernst current is described by the same diagrams in Fig. 5, with corresponding external vertices. Here we have

$$\mathbf{j}_N^{(a)}=\frac{2e^2M}{m}T\sum_{\omega_k}\int(dq)(\mathbf{A}_H\mathbf{q})(\mathbf{A}_q\mathbf{k})\mathbf{q}B_1B_3L(\mathbf{q},\omega_k+\Omega_v)$$
$$\times L(\mathbf{q}+\mathbf{k},\omega_k+\Omega_v)L(\mathbf{q},\omega_k), \qquad (23)$$

where

$$(\mathbf{A}_q\mathbf{k})B_3=T\sum_{\varepsilon_n}\int(dp)\xi_pG(\mathbf{p}+\mathbf{k},\varepsilon_n+\Omega_v)G$$
$$\times(\mathbf{p},\varepsilon_n)G(\mathbf{q}-\mathbf{p},\omega_k-\varepsilon_n)(\mathbf{A}_q\mathbf{v}). \qquad (24)$$

The block B_3 was calculated in Ref. 9; the result is

$$B_3=\frac{i\rho v_F^2}{64T_c}-\frac{1}{16\pi}\left[\frac{\partial(\rho v^2)}{\partial\varepsilon}\right]_{\varepsilon_F}\ln\frac{\omega_D}{2\pi T_c} \qquad (25)$$

(ω_D is the Debye frequency). In calculating the correction to the Nernst coefficient, we do not need to expand ρv^2 in order to obtain a null result, so we are interested in only the first term in (25). Evaluating the contribution of the second diagram in Fig. 5 in a corresponding way, we find

$$\mathbf{j}_N=-\frac{i\cdot7\zeta(3)}{256}\frac{e^2v_F^4\rho^2}{mT_c^3}\mathbf{A}_H(\mathbf{A}_q\mathbf{k})$$
$$\times T\sum_{\omega_k}\int(dq)\mathbf{q}_\parallel^2[L^2(\mathbf{q},\omega_k+\Omega_v)L(\mathbf{q},\omega_k)$$
$$-L(\mathbf{q},\omega_k+\Omega_v)L^2(\mathbf{q},\omega_k)]. \qquad (26)$$

As a result, the relative fluctuational correction to the Nernst coefficient is [here we are using (9)]

$$\frac{N^{(fl)}}{N^{(n)}}=\frac{\pi^3}{96\cdot7\zeta(3)}\frac{1}{(T_c\tau)^2}\frac{1}{\varepsilon_F\tau}F\left(\frac{T-T_c}{T_c},\delta_0^2\right). \qquad (27)$$

Since the Ettinghausen coefficient is proportional to the Nernst coefficient ($B=NT$) according to the Onsager relations for the kinetic coefficients, we have

$$\frac{B^{(fl)}}{B^{(n)}}=\frac{N^{(fl)}}{N^{(n)}}. \qquad (28)$$

We turn now to the Righi–Leduc effect. Noting that both external vertices correspond to the heat-flux operator, we find that the contribution of the first diagram in Fig. 5 to the heat flux is

$$\mathbf{q}^{(a)}=\frac{2eM}{m}T\sum_{\omega_k}\int(dq)(\mathbf{A}_H\mathbf{q})(\mathbf{A}_q\mathbf{k})\mathbf{q}B_3B_4L(\mathbf{q},\omega_k+\Omega_v)$$
$$\times L(\mathbf{q}+\mathbf{k},\omega_k+\Omega_v)L(\mathbf{q},\omega_k), \qquad (29)$$

where

$$(\mathbf{A}_q\mathbf{k})B_4=T\sum_{\varepsilon_n}\int(dp)\xi_pG(\mathbf{p}+\mathbf{k},\varepsilon_n+\Omega_v)G$$
$$\times(\mathbf{p},\varepsilon_n)G(\mathbf{q}-\mathbf{p},\omega_k-\varepsilon_n)(\mathbf{A}_q\mathbf{v}). \qquad (30)$$

For the block B_4 we find

$$B_4=B_3.$$

To find a null result we need to consider the second term in

(25), obtained as a result of the expansion. The total heat flux is

$$\mathbf{q}=-\frac{i}{\pi 2^9}\frac{ev_F^2\rho}{mT_c}\left[\frac{\partial(\rho v^2)}{\partial\varepsilon}\right]_{\varepsilon_F}\ln\frac{\omega_D}{2\pi T_c}\mathbf{A}_H(\mathbf{A}_e\mathbf{k})$$

$$\times T\sum_{\omega_k}\int(dq)\mathbf{q}_\parallel^2[L^2(\mathbf{q},\omega_k+\Omega_v)L(\mathbf{q},\omega_k)$$

$$-L(\mathbf{q},\omega_k+\Omega_v)L^2(\mathbf{q}.\omega_k)]. \quad (31)$$

As a result we find

$$\frac{L^{(fl)}}{L^{(n)}}=\frac{\pi^2}{128[7\zeta(3)]^2}\ln\frac{\omega_D}{2\pi T_c}\frac{1}{T_c\tau}\frac{1}{\varepsilon_F\tau}F\left(\frac{T-T_c}{T_c},\delta_0^2\right). \quad (32)$$

The temperature dependence of the fluctuational corrections to the coefficients N, B, and L is the same as that of the correction to the Hall conductivity.

7. CONCLUSION

As we mentioned back in the Introduction, experiments on the high T_c superconductors reveal an anomalous behavior of the Hall conductivity and also of the Nernst, Ettinghausen, and Righi–Leduc coefficients in the fluctuation region. The basic results of this study [expressions (21), (27), (28), and (32)] are the relative fluctuational corrections to the electron components of these coefficients. It can be seen from these expressions that as T_c is approached from above one should observe an increase in the coefficients σ_H, N, B, and L because of the fluctuational corrections found here. Since the results were derived in first-order perturbation theory in the superconducting fluctuations, the power-law growth in the immediate vicinity of T_c is limited by the contributions of the following orders. In addition, one should bear in mind the nonuniformity of the sample, which leads to a smearing of the transition temperature and also of the fluctuation effects. It is thus clear that the increase in the coefficients which results from the fluctuational corrections found here comes to a halt in the immediate vicinity of the transition point. In the cases of the Hall, Nernst, and Ettinghausen coefficients, where the electron component appears to be predominant, we would expect to find a peak near T_c. For the Righi–Leduc coefficient, as for the thermal conductivity in the absence of the magnetic field, the electron component is superposed on a large component of different origin (apparently of phonon origin), which leads to a peak at $T\approx 60$ K. In this case the effect of the fluctuations is not as obvious: It is seen as the beginning of an increase in the coefficient a few degrees above T_c.

We have calculated the fluctuational corrections only for temperatures above the transition temperature, but it is clear that as T_c is crossed these corrections will vanish algebraically with decreasing temperature. Estimates from (21), (27), (28), and (32) show that at temperatures 10–12 K above T_c the fluctuational correction to the Nernst and Ettinghausen coefficients is already comparable to the main contribution [(9), from electron-impurity scattering] in the case of the high T_c superconductors. The relative fluctuational corrections to the Hall and Righi–Leduc coefficients reach 25–30% at these temperatures.

Our results show that the fluctuational corrections to the kinetic coefficients describing transport in a weak magnetic field are more singular in the degree of proximity to T_c than are the corrections to the thermal and electrical conductivities and the thermal emf calculated previously for the case without a magnetic field.[9,17] The reason is that diagrams analogous to the Aslamazov–Larkin diagram arise when there is a magnetic field. In these diagrams, one of the fluctuational propagators is cut in two by a vertex describing the interaction of the electrons with the magnetic field. This "extra" propagator gives rise to an additional power of $T-T_c$ in the denominator of the expressions for the corrections to the kinetic coefficients. It thus leads to a substantial increase in the relative corrections in comparison with the corrections to the corresponding coefficients in the absence of a magnetic field. This conclusion is in agreement with the experimental data reported by Gridin *et al.*,[4] who measured the temperature dependence of the difference between the thermal emf values measured in the presence and absence of a magnetic field. Gridin *et al.*[4] found that imposing a magnetic field results in a pronounced increase in the thermal emf near T_c.

The fluctuational correction to the Hall conductivity was calculated previously, by Fukuyama *et al.*,[18] for the case of a dirty superconductor and an isotropic electron spectrum. As a result, Fukuyama *et al.*[18] found the same temperature dependence for the fluctuational correction as in the limiting cases in (21). However, we believe that a coefficient in that functional dependence was calculated incorrectly. The reason is that the small factor $\sim T/\varepsilon_F$ required for obtaining a nonvanishing result for the Hall conductivity was extracted from the fluctuation propagator alone in Ref. 18. Our own calculations show that such terms cancel out, so the corrections required arise only from an expansion of ρv^2 in blocks of Green's function. Ullah and Dorsey[19] calculated the fluctuational correction to the Ettinghausen coefficient for magnetic fields close to H_{c2}, in contrast with our calculations for weak fields. The method which they[19] used to incorporate the interaction of fluctuations in the Hartree approximation makes it possible to derive an expression for the fluctuational corrections in the immediate vicinity of T_c, where we can no longer restrict the analysis to a first-order perturbation theory in the superconducting fluctuations.

We are deeply grateful to A. V. Ustinov for calling our attention to the need for an analysis of this question.

[1)] This assumption does not limit the generality of the analysis if, for arbitrary orientations of **E**, **H**, and ∇T, we consider only the projection of the magnetic field onto the c axis and only the projections of the electric field and the temperature gradient onto the ab plane.

[1] Zhao Kong, Zhang Qirvi, Kuan Weiyan *et al.*, Solid State Commun. **64**, 885 (1987).
[2] L. Forro, M. Raki, J. Y. Henry *et al.*, Solid State Commun. **69**, 1097 (1989).
[3] S. Ikegawa, T. Wada, A. Ichinose *et al.*, Phys. Rev. B **41**, 11673 (1990).
[4] V. V. Gridin, P. Pernambuco-Wise, C. G. Trendall *et al.*, Phys. Rev. B **40**, 8814 (1989).
[5] M. Galffy, A. Freimuth, and U. Murek, Phys. Rev. B **41**, 11029 (1990).
[6] M. Zeh, H.-C. Ri, F. Kober *et al.*, Phys. Rev. Lett. **64**, 3195 (1990).
[7] T. T. M. Palstra, B. Batlogg, L. F. Schneemeyer, and J. V. Waszczak, Phys. Rev. Lett. **64**, 3090 (1990).
[8] G. Strinati and C. Castellani, Phys. Rev. B **36**, 2270 (1987).
[9] A. A. Varlamov and L. V. Livanov, Zh. Eksp. Teor. Fiz. **98**, 584 (1990) [Sov. Phys. JETP **71**, 325 (1990)].

[10] C. Di Castro, C. Castellani, R. Raimondi, and A. A. Varlamov, Phys. Rev. B (in press).
[11] B. L. Altshuler, D. Khmel'nitzkii, A. I. Larkin, and P. A. Lee, Phys. Rev. B **22**, 5142 (1980).
[12] B. L. Altshuler and A. G. Aronov, in *Electron–Electron Interaction in Disordered Systems* (ed. A. L. Efros and M. Pollak), Oxford, New York, 1985, p. 1.
[13] A. A. Abrikosov, *Fundamentals of the Theory of Metals*, Nauka, Moscow, 1987 (North-Holland, Amsterdam, 1988).
[14] R. Kubo, M. Yokota, and S. Nakayuma, J. Phys. Soc. Jpn. **12**, 1203 (1957).
[15] R. Kubo, J. Phys. Soc. Jpn. **12**, 570 (1957).
[16] L. G. Aslamozov and A. A. Varlamov, J. Low Temp. Phys. **38**, 223 (1980).
[17] L. G. Aslamazov and A. I. Larkin, Fiz. Tverd. Tela (Leningrad) **10**, 1104 (1968) [Sov. Phys. Solid State **10**, 875 (1968)].
[18] H. Fukuyama, H. Ebisawa, and T. Tsuzuki, Progr. Theor. Phys. **46**, 1028 (1971).
[19] S. Ullah and A. T. Dorsey, Phys. Rev. Lett. **65**, 2321 (1990).

Translated by D. Parsons